CONF-870142--14

DE87 011483

THE FERMI SURFACE OF CeSb

G. W. Crabtree, H. Aoki,* W. Joss,** and F. Hulliger†

Materials Science Division

Argonne National Laboratory,†† Argonne, Illinois 60439

April 1987

DISCLAIMER

Submitted to 5th International Conference on Valence Fluctuations, January 5-9, 1987, Bangalore, India.

*National Research Institute for Metals, 2-3-12 Nakameguro, Meguroku, Tokyo 153, Japan.

**Max Planck Institute, BP 166X, Grenoble 38042, France.

†Laboratorium fur Festkorperphysik, ETH, Zurich, Switzerland.

††Work supported by the U.S. Department of Energy, BES-Materials Sciences, under Contract #W-31-109-ENG-38.

5th International Conference on Valence Fluctuations
5-9 January 1987 Bangalore, India

THE FERMI SURFACE OF CeSb

G. W. Crabtree, H. Aoki,* W. Joss,** and F. Hulliger***
Materials Science and Technology Division
Argonne National Laboratory
Argonne, IL, 60439

INTRODUCTION

A central issue of f-electron metals is the importance and description of hybridization between the f and conduction electrons. The strength of the hybridization controls the general nature of the behavior:[1,2] strong hybridization leads to purely itinerant behavior with properties similar to those of the transition metals, weak hybridization leads to narrow band behavior which is manifested in mixed valence , heavy fermion and Kondo lattice behavior as the hybridization decreases, and in the limit of zero hybridization the f-electron localizes leading to a well defined moment and magnetic order at low temperature. Although band theory provides a full description of hybridization for the itinerant[3] and, to a certain extent, mixed valence[4] and heavy fermion[5,6] metals, the precise nature and description of hybridization near the local end of the spectrum is not well understood.

CeSb is an excellent metal in which to test models of hybridization. It displays a large number of magnetic phases as a function of temperature and field, indicating that there is a delicate balance between positive and negative exchange interactions between Ce ions. The semimetallic Fermi surface consists of closed sheets of electrons and holes which can be well described by band theory. Because the effective masses are low, the entire Fermi surface can be observed with the de Haas-van Alphen effect to high accuracy. Comparison with LaSb where there is no f electron provides insight into the effect of the f electron on the Fermi surface properties. Furthermore, there has been a large body of experimental work on the magnetic structure[7], crystal field effects[8], and magnetic properties[9] and a great deal of theoretical work[10] on the exchange interaction,[11,12] ordering mechanisms,[13,14] and electronic structure[15,16] to provide the necessary details for a realistic analysis of models.

In this paper we use accurate Fermi surface measurements as a test of hybridization models in CeSb. We present detailed measurements of the Fermi surface geometry and effective masses which show a number of unusual properties associated with the magnetic structure and anisotropy. We compare our measurements with predictions of a band structure in which the f-electron is assumed to be local, interacting with the conduction electrons only through anisotropic Coulomb and exchange interactions. This model reproduces all the unusual

features observed in the measurements and suggests that hybridization is not essential to describing the electronic properties of CeSb.

MAGNETIC PROPERTIES OF CeSb

CeSb exhibits at least 15 magnetic phases[7] as a function of temperature and field. The low temperature phases consist of stacks of ferromagnetically aligned (100) planes where the Ce has a full moment of 2.06 μ_B pointing either parallel or anti-parallel to the <100> direction. The magnetic structures can be described as a stacking sequence of moment directions. Below 7 K there are four different structures as the field increases: ++--, ++--++-, ++-, and +. The moments in these three phases are pinned very strongly along the <100> direction. Magnetization measurements[17] indicate that the anisotropy field necessary to saturate the moment in the <110> direction is over 100 T. This strong anisotropy persists even in the paramagnetic state, implying that it is due to single ion effects rather than to the exchange interaction.

The strong magnetic anisotropy leads to dramatic domain effects in the presence of an external magnetic field. In the absence of a field, the moment is equally likely to point along any of the three crystallographically equivalent <100> directions. In a field the magnetic energy is lowered if the moment chooses to point along the <100> direction closest to the applied field direction, resulting in a single domain sample. As the field direction changes relative to the crystal, the favored domain direction may suddenly change from one <100> type direction to another. As will be explained below, this change in the magnetization direction with field direction has dramatic consequences for the symmetry of the observed Fermi surface.

EXPERIMENTAL RESULTS

dHvA measurements were taken in fields up to 15 T and at temperatures as low as 0.4 K by the field modulation technique. Spherically shaped samples were used to avoid field inhomogeneity due to a variation of the demagnetizing field over the sample volume. Strong signals were observed in both the high field induced paramagnetic phase (+) and the intermediate field antiferromagnetic phase (++-). The Fermi surface changes significantly between these two phases, as shown by the field sweep data in Figure 1. Large low frequency oscillations in the high field region are abruptly replaced by smaller amplitude higher frequency oscillations in the low field region. The field at which the phase transition takes place can be accurately determined from its effect on the dHvA oscillations. From data such as this we have measured the transition field for all directions in the (100) and (110) symmetry planes. This data is shown in Figure 2, where a clearly discernable hysteresis between the increasing and decreasing field transition showing the first order nature of the transition can be seen. Domain effects are also evident in the sharp cusp in the transition field occuring at <111>. For field directions between <001> and <111> in the (-110) plane and between <001> and <101> in the (100) plane the favored magnetization direction is <001>. However for directions between <111> and <110> in the (-110) plane the favored direction switches to either <010> or <100>. The cusp at <111> reflects this switch in the magnetic domain. The strong magnetic anisotropy can also be seen in the shape of the transition field curve. The solid line in Figure 2 is of the form $H_0/\cos\theta$ where θ is the angle between the field and the closest <100> type direction. The excellent fit of this curve to the transition field implies that for an arbitrary direction the transition occurs whenever the component of the field along the closest <100> direction equals H_0. This behavior is expected if the moment is

pinned along the closest <100>.

The dHvA frequencies as a function of angle in the (100) and (110) planes are shown in Figure 3. These data are more extensive than the earlier data of Kitazawa, et al.[18] Qualitatively, the frequencies may be interpreted by a simple model Fermi surface consisting of three hole ellipsoids centered at Γ and a set of electron ellipsoids at X as shown in Figure 4. (As described below, band structure calculations show that in CeSb the ellipsoids are centered along the Γ-X line rather than at X as in LaSb.) The β orbits are due to the holes and the γ orbits are due to the ellipsoids. Although the β_1 orbit is not observed across the entire (110) plane we believe it exists everywhere but is simply too weak to see near <111>. The α and 2α branches cannot be interpreted by the model of Figure 4 and require special comment. The 2α branch appears at first to be part of the X ellipsoids, completing the low frequency branch of the γ orbits. However careful analysis of the angular dependence of the frequency and mass data shows that 2α is the second harmonic of the low frequency branch α. The α orbit itself has the right shape to complete the γ pattern, but its magnitude is too small by approximately a factor of two. As we show below, the cusp in the shape of the α orbit at <111> is due to domain switching and the difference in magnitude between the α and γ orbits is due to the moment on the Ce ion breaking the cubic symmetry of the chemical unit cell.

The effective masses of the orbits shown in Figure 3 are given in Table 1. The masses are all rather small, the largest being 1.00.

WEAK COUPLING MODEL

The f electron in CeSb can affect the conduction states in two ways: through the crystal potential due to its Coulomb and exchange interaction (as in the standard rare earth model), or through direct hybridization. The anomalous properties of Ce and U compounds are often attributed completely to hybridization, leaving other mechamisms unexplored. However the f electron can affect the conduction states through its exchange and Coulomb interactions without participating in hybridization. These effects are usually more subtle than those of direct hybridization and often are only of secondary importance if significant hybridization exists. Near the local end of the f electron spectrum, both hybridization and crystal potential effects may play a role, and it is not easy to separate the two mechanisms experimentally.

In what follows we examine the crystal potential effects in CeSb and show that our dHvA data can be quantitatively interpreted assuming the f electron is purely local without invoking hybridization. CeSb is an especially good metal for such a model because there is enough experimental information available to specify the f electron orbital and spin state. This information combined with a band structure calculation for the conduction electron properties gives a detailed description of the electronic structure of the metal. The completeness of the experimental Fermi surface geometry and effective mass information allows a detailed and thorough test of the predictions of the model.

The details of the "weak coupling" model were developed by Norman and Koelling.[15] There are three basic assumptions.

1) The f electron is in a local atomic-like state with j=5/2 and μ=-5/2. The atomic state is chosen to give a moment equal to that observed in magnetization experiments

2) The quantization axis points along a <100> type direction no matter what the direction of the applied field. This condition leads to the strong magnetic anisotropy observed in both the paramagnetic and ordered states.

3) There is no hybridization. The f electron affects the conduction electron only through its Coulomb and exchange interactions.
With these assumptions and a band calculation, the model for the electronic structure is completely determined. The detailed dispersion curves, the symmetry of the states, the band masses and the Fermi surface geometry can be calculated. Essentially the f electron is treated as a partially filled core state whose crystal potential is determined in the usual way. There are a number of subtleties and approximations[15] in carrying out the calculation which will not be treated here. We summarize the results and give a physical discussion of their significance.

An important feature of the weak coupling model is the breaking of the chemical cubic symmetry by the f electron orbital. The j=5/2, μ=-5/2 charge distribution is shaped like an oblate spheroid so that with the quantization axis along <001> each Ce site has a pancake shaped charge distribution oriented along the z axis. The associated magnetic moment also points along z with the spin and orbital contributions in opposite directions. The z direction is then clearly different from the x and y directions both electrostatically and magnetically, reducing the symmetry of the crystal potential from cubic to tetragonal. This allows the Fermi surface to distort from cubic symmetry and, when coupled with the domain switching effects caused by the strong magnetic anisotropy, provides the explanation of the unusual shape and placement of the α orbit in the dHvA data.

DISCUSSION

The results of the weak coupling model can be qualitatively understood by comparison with the non-f metal LaSb. In LaSb[15,16] there are two hole sheets at Γ and a set of electron ellipsoids at X. The hole sheets arise mainly from the Sb p bands and the ellipsoids from the La d bands. The addition of the localized f electron via the weak coupling model has a large effect on the band structure. A third hole sheet appears at Γ due to modified spin orbit effects in agreement with experiment. In addition, the ellipsoids at X are significantly affected by the potential due to the local f charge density. This is to be expected because the ellipsoid wave functions are mainly of Ce d character and therefore sample the charge on the Ce site more fully than do the Sb p like wave functions of the holes. All three of the ellipsoids are shortened in their long direction so that they no longer include the X point and are centered along the Γ-X line. Because of the anisotropy of the f charge distribution, the ellipsoids in the x-y plane are distorted differently than the ellipsoid along the z axis. The z axis ellipsoid shrinks in size while the x-y ellipsoids grow. This pattern can be qualitatively understood by considering the local f charge density as a perterbation acting on the d-like states near X. In cubic symmetry the states associated with each of the three ellipsoids are degenerate in energy, even though the spatial saymmetry of their wavefunctions is different. The tetragonal symmetry of the perturbation splits this degeneracy, shifting the states associated with the k_z ellipsoid up in energy and those associated with the k_x and k_y ellipsoids down in energy. This band shifting leads to the changes in the size of the ellipsoids illustrated in Figure 5.

The differing sizes of the ellipsoids in the weak coupling model of CeSb explains the separation in frequency between the γ and α branches in Figure 3. The smaller ellipsoid whose axis is along the moment direction gives rise to the α orbit while the larger ellipsoids produce the γ branches. The cusp in the α branch at <111> is due to the domain switching effect. For field directions between <001> and <111> the moment direction and the tetragonal axis are along <001>. At <111> all three <100> type directions are equivalent and any is equally likely to be chosen as the moment direction. For fields between <111> and <110> the <010> and

<100> directions are closer to the field direction than is <001> and the moment switches to one of them. The tetragonal direction follows the moment, so the Brillouin zone has effectively rotated 90° and the small ellipsoid is now oriented in a different direction relative to the field, as illustrated in Figure 5. For field directions between <111> and <110> all three ellipsoids are non-degenerate and three distinct branches can be seen in the data.

The effective masses observed in the ferromagnetic phase are shown in Table 1. As can be seen, the masses are rather light, all being less than 1.0. These low masses suggest wide bands with little f electron admixture. This picture is supported by the weak coupling model, which predicts masses about a factor of 1.5-2 lower than those observed. This difference is naturally explained by the electron-phonon enhancement which is of the same order of magnitude as that in LaSb.

The results of the weak coupling model are qualitatively quite different from what would be expected from a hybridization model. Because the f electron cannot hybridize with d electrons on the same Ce site it will mix mainly with the p states on neighboring Sb atoms. These states produce the hole surfaces at Γ. Therefore hybridization will primarily affect the Γ-centered surfaces rather than the ellipsoids. The domain switching effects that occur at <111> should then introduce cusps in the β orbits as their tetragonal axis switches from <001> to <100> or <010>. Since no such switching effects are seen, the hybridization mechanism is unlikely. In addition, hybridization would introduce f character into the conduction states narrowing the bands and increasing the masses. Since the masses are not large and are explainable in terms of the weak coupling model, there is little evidence for hybridization.

CONCLUSION

We have presented here a description of the f electron behavior in CeSb in terms of a localized f model. Such a model has not been examined in detail because the anomalous behavior in CeSb was conventionally attributed to 4f hybridization. However, as we have shown above, the crystal potential due to the Coulomb and exchange interactions of the incomplete 4f shell in Ce has dramatic and extensive effects on the Fermi surface properties of CeSb. These effects can be explored in detail in CeSb because there is complete and accurate Fermi surface information from experiment and well- defined quantitative models of the electronic structure in which the effects of crystal potential and hybridization can be analysed separately. For most properties other than the Fermi surface, it is not possible to take sufficiently detailed experimental information to distinguish a local f picture from a hybridized picture. Thus for properties such as crystal field splittings, magnetic anisotropy, ordering temperature and magnetic structure the role of hybridization can not be easily separated from the role of the crystal potential. For some of these properties, however, it is possible to propose models based soley on crystal potential effects and test their ability to describe experiment. One such model for the strong magnetic anisotropy of CeSb is a natural extension of the weak coupling model described above. In this picture, the strong anisotropy is due to the variation of the total electronic energy with the quantization axis of the f orbital on Ce. This proposal can be tested within the framework of the weak coupling model by calculating the total electronic energy for several orientations of the quantization axis. A strong increase in the total energy with angle away from <001> would lead to the observed strong anisotropy. This proposal is similar in spirit to an earlier suggestion of Kasuya, et al.[19] that links the magnetic anisotrpy to the total electronic energy, except here the 4f moment-conduction electron interaction is strictly through the crystal potential and does not involve any hybridization. Like the Fermi surface models discussed above, this model for the

magnetic anisotropy is fully defined and can be quantitatively calculated to give an unambiguous prediction. It also contains enough flexibility to allow CeSb to be anomalous compared to the other RESb compounds, since the local 4f orbitals in these cases contain two or more electrons and the crystal potential arising from them may be expected to be different from that in CeSb.

The data and interpretation we have presented above shows that the Fermi surface properties of CeSb can be well described in a purely local model where no 4f hybridization is included. We recognize that for some properties such as magnetic ordering or the RKKY interaction some hybridization may be important. However, we emphasize that hybridization is not a necessary feature of all Ce compounds, and that more conventional local pictures which can be quantitatively analysed may provide alternate explanations. The picture we have developed for CeSb can be applied to any of the Ce compounds near the local end of the spectrum and demonstrates that crystal potential effects can play a dominant role in producing anomalous behavior.

We thank M. R. Norman and D. D. Koelling for many stimulating discussions. Argonne National Laboratory is operated by the U. S. Department of Energy, BES-Materials Sciences, under contract W-31-109-Eng-38.

REFERENCES

* National Research Institute for Metals, 2-3-12 Nakameguro, Megureku, Tokyo 153, Japan
** Max Planck Institute, BP 166X, Grenoble 38042, France
*** Laboratorium fur Festkorperphysik, ETH, Zurich, Switzerland

1. D. D. Koelling, B. D. Dunlap, and G. W. Crabtree, Phys. Rev. B31:4966 (1985).
2. G. W. Crabtree, J. Mag. Mag. Mat. 52:169 (1985).
3. A. J. Arko, D. D. Koelling, and J. E. Schirber, in: Handbook of the Physics and Chemistry of the Actinides, A. J. Freeman and G. H. Lander, eds., vol. 2, North Holland, Amsterdam (1985).
4. D. D. Koelling, Solid State Commun. 43:247 (1982)
5. M. R. Norman, these proceedings.
6. D. D. Koelling, M. R. Norman, and A. J. Arko, J. Mag. Mag. Mat. 63&64:638 (1987)
7. J. Rossat-Mignod, J. M. Effantin, P. Burlet, T. Chattopadhyay, L. P. Regnault, H. Bartholin, C. Vetteir, O. Vogt, D. Ravot, and J. C. Achart, J. Mag. Mag. Mat. 52:111 (1985).
8. H. Heer, A. Furrer, W. Halg and O. Vogt, J. Phys. C:Solid State Phys. 12:5207 (1979).
9. F. Hulliger and H. R. Ott, Z. Phys. B 29:47 (1978).
10. H. Takahashi and T. Kasuya, J. Phys. C:Solid State Phys. 18:2697 (1985) and following papers.
11. P. Thayamballi and B. R. Cooper, Phys. Rev. B31:5911 (1985).
12. H. Takahashi and T. Kasuya, J. Phys. C:Solid State Phys. 18:2755 (1985).
13. B. R. Cooper and R. Siemann, in: Proceedings of the International Conference on Crystalline Electric Field and Structural Effects in f-electron Systems, J. E. Crow, R. P. Guertin and T. Mihalisin, ed.,Plenum, New York (1972).
14. H. Takahashi and T. Kasuya, J. Phys. C:Solid State Phys. 18:2731 (1985).
15. M. R. Norman and D. D. Koelling, Phys. Rev. B 33:6730 (1986).
16. T. Kasuya, O.Sakai, J. Tanaka, H. Kitazawa and T. Suzuki, J. Mag. Mag. Mat. 63&64:9 (1987).
17. P. Burlet, J. Rossat-Mignod, H. Bartholin and O. Vogt, J. Physique 40:47 (1979).

18. H. Kitazawa, T. Suzuki, M. Sera, I. Oguro, A. Yanase, A. Hasegawa and T. Kasuya, J. Mag. Mag. Mat. 31-34:421 (1983).
19. H. Takahashi and T Kasuya, J. Phys. C:Solid State Phys. 18:2731 (1985).

Table 1. Effective masses in CeSb measured by the dHvA effect and calculated by the weak coupling model. The two masses given for the weak coupling model refer to spin up and spin down orbits.

Orbit	Field direction	Experimental mass	Weak coupling mass
α	<001>	0.23	0.17, 0.13
α	<110>	0.31	0.19, 0.25
β_1	<001>	0.50	0.17, 0.18
β_2	<001>	0.97	0.30, 0.31
β_2	<110>	0.56	0.30, 0.30
β_3	<001>	0.89	0.53, 0.61
β_3	<110>	0.65	0.40, 0.45
γ_l	<110>	0.49	0.30, 0.33
γ_l	<111>	0.53	0.35, 0.37
γ_h	<001>	0.94	0.56, 0.56
γ_h	<110>	1.00	0.60, 0.67
γ_h'	<001>	0.82	0.56, 0.56
γ_h'	<110>	0.90	0.60, 0.67

Figure Captions

Figure 1. dHvA oscillations on the high and low field side of the magnetic phase transition from ++- to +.

Figure 2. Transiton field between the ++- and + phases as a function of angle in the (100) and (110) symmetry planes

Figure 3. dHvA frequencies as a function of angle in the (100) and (110) planes.

Figure 4. Schematic model of the Fermi surface of LaSb or CeSb without the f electron.

Figure 5. Ellipsoidal sheet of the Fermi surface of CeSb for the field in the

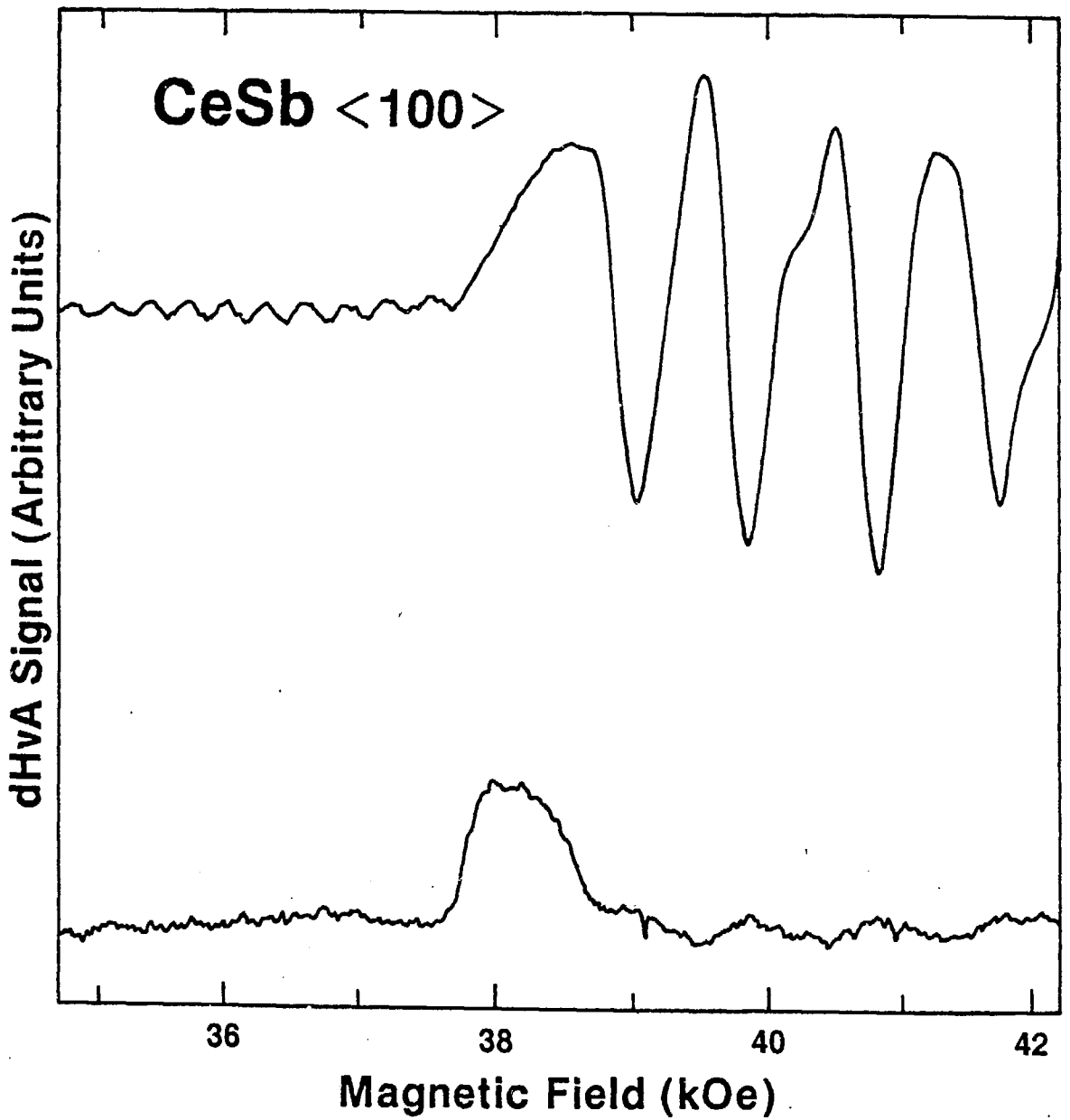
CeSb <100>
dHvA Signal (Arbitrary Units)
36
38
40
42
Magnetic Field (kOe)

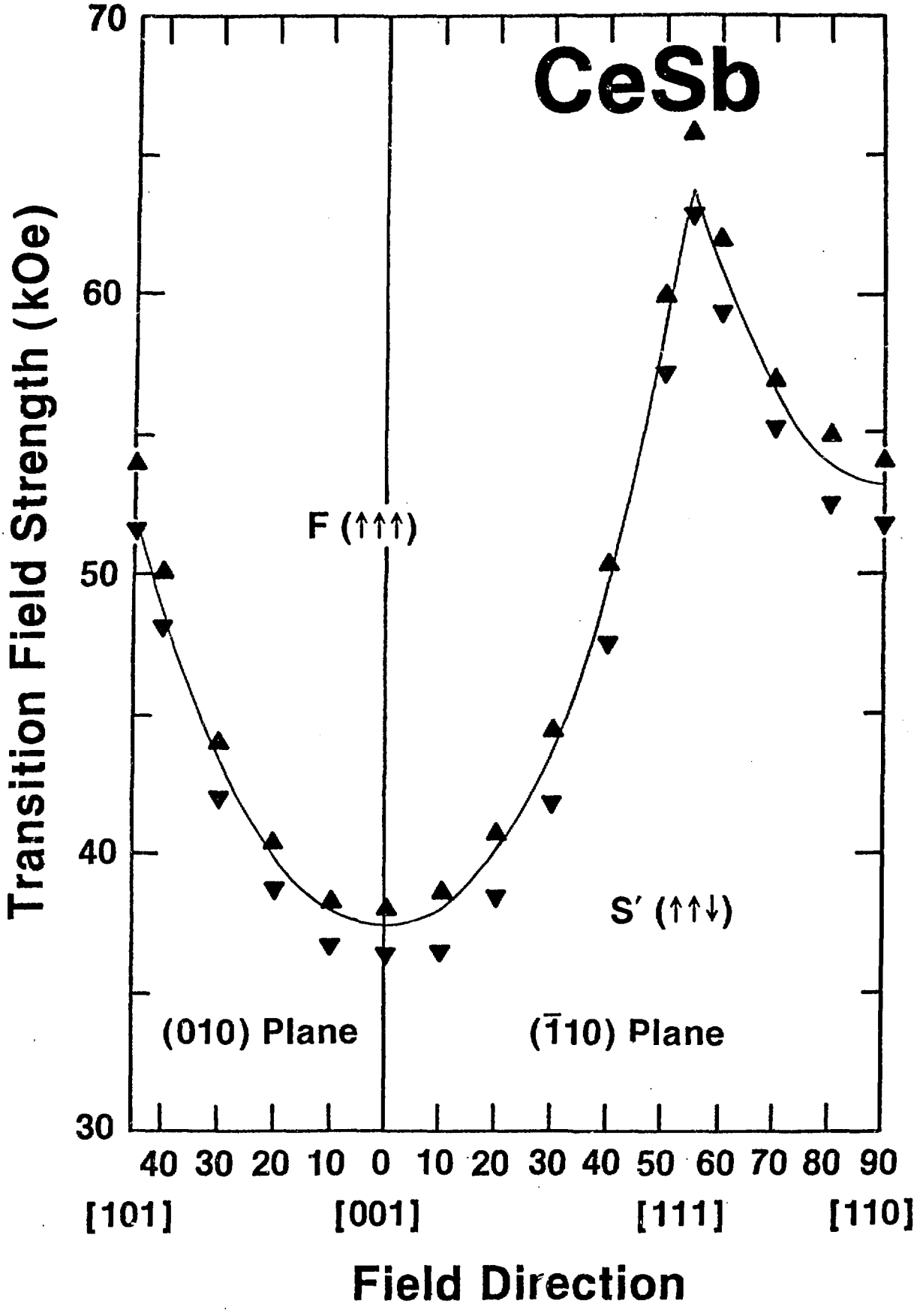
CeSb
Transition Field Strength (kOe)
70
60
50
40
30
F (↑↑↑)
S′ (↑↑↓)
(010) Plane
(1̄10) Plane
40 30 20 10 0 10 20 30 40 50 60 70 80 90
[101]
[001]
[111]
[110]
Field Direction

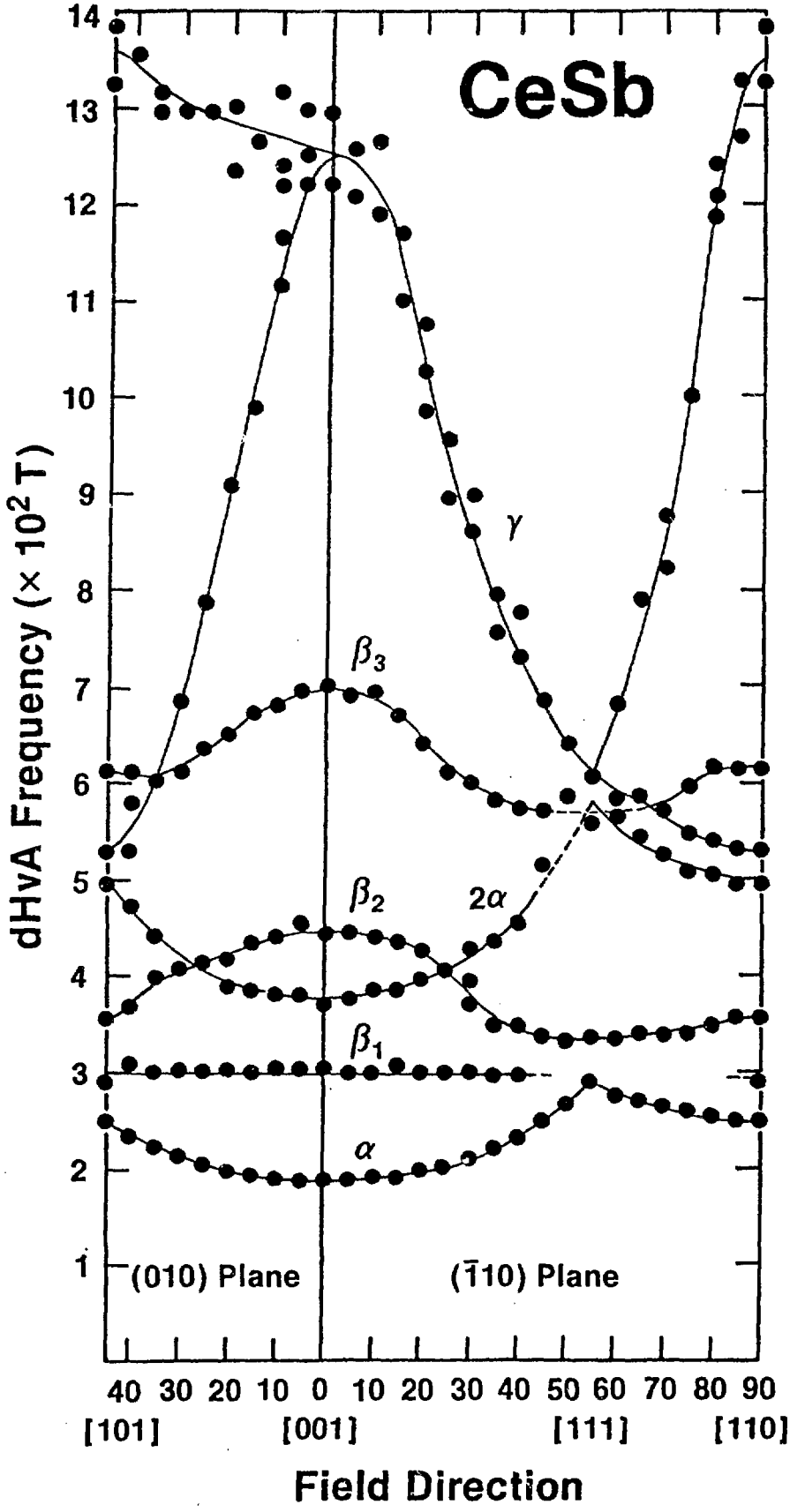
CeSb
dHvA Frequency (× 10² T)
14
13
12
11
10
9
8
7
6
5
4
3
2
1
γ
β3
β2
2α
β1
α
(010) Plane
(1̄10) Plane
40 30 20 10 0 10 20 30 40 50 60 70 80 90
[101]
[001]
[111]
[110]
Field Direction

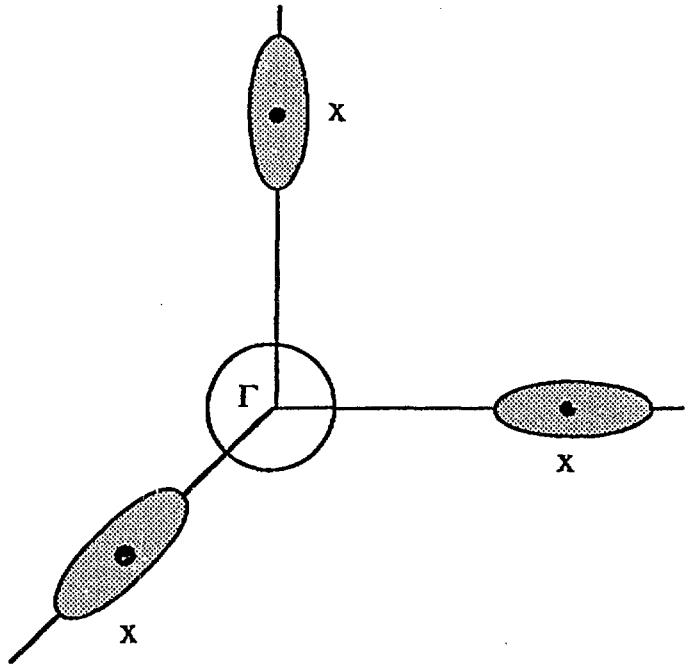

Fig. 4 Schematic model of the Fermi surface of LaSb or CeSb without the f electron.

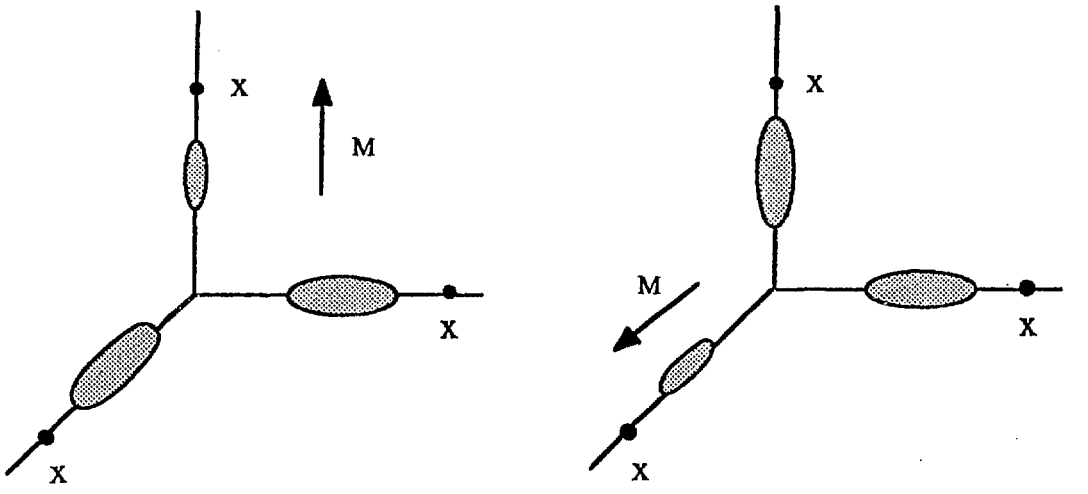

Fig. 5 . Ellipsoidal sheets of the Fermi surface of CeSb for the moment in the <001> and <100> directions.